Journal of Statistical Physics, Vol. 42, Nos. 1/2, 1986

Activated Barrier Crossing: Comparison of Experiment and Theory

Graham R. Fleming,[1,2] Scott H. Courtney,[1] and Michael W. Balk[1]

Received July 11, 1985

Photochemical isomerization in stilbene and diphenyl butadiene has been studied as a model for activated barrier crossing. Experiments have been carried out from isolated molecule conditions up to 3000 atm pressure in solution-phase samples. The qualitative features predicted by Kramers theory are observed. The system undergoes a transition from energy-controlled to diffusion-controlled behavior in the high-pressure gas phase. The influences of multidimensionality, intramolecular vibrational relaxation, and frequency dependent friction are discussed.

KEY WORDS: Photochemical isomerization; Kramers' equation; Kramers' turnover; frequency-dependent friction; intramolecular vibrational relaxation; barrier crossing; rovibrational density of states.

1. INTRODUCTION

Photochemical isomerization (Fig. 1) provides a practical testing ground for theories of activated barrier crossing, an essential ingredient of descriptions of solution phase chemical reactions. The fact that isomerizations occur in the excited state means that the process can be readily initiated by a short optical pulse of light and the decay of population of the initial isomer, or build-up of final isomer, followed by optical means. We have selected systems for study where the isomerization rates are relatively slow compared to vibrational or solvent relaxation processes in solution. We have also chosen systems in which the moving group is fairly large compared to the size of the solvent molecules (except for the more viscous

[1] Department of Chemistry and The James Franck Institute, The University of Chicago, Chicago, Illinois 60637.
[2] Camille and Henry Dreyfus Teacher Scholar.

0022-4715/86/0100-0083$05.00/0

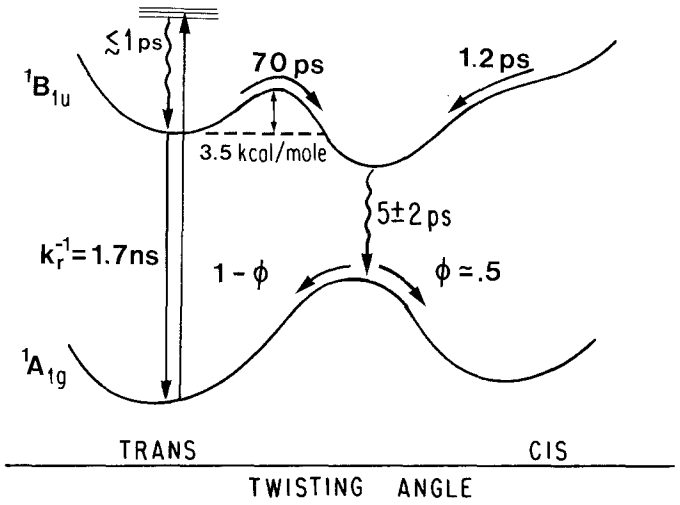

Fig. 1. Summary of stilbene isomerization dynamics in hexane at room temperature. The rate of decay of the twisted conformation to the ground state surface is $(5 \pm 2 \text{ psec})^{-1}$ (B. I. Green, private communication). The decay rate for the *cis* isomer was determined in Ref. 62 and the branching ratio in Refs. 63 and 64.

solvents) so that a continuum hydrodynamic approximation to the solvent friction stands the best chance of applying. The use of an excited state process has the disadvantage that other nonradiative processes may compete with the isomerization and distort the viscosity dependence at high viscosity. We have carefully investigated the rates of these other processes in some cases,[1] and in one case studied isomerization of the excited state surface and the return isomerization on the ground state surface.[2] In this latter case there can be no competing processes and we found qualitatively identical behavior to that in the excited state. A further possible complication in excited state processes is that the potential surface on which isomerization occurs may be quite sensitive to the environment.

In this paper we describe experiments on several systems studied over a wide range of densities, from isolated molecule conditions to pressures of 3000 atm and over a temperature range of 150 K. The wide range of conditions allow detailed comparisons with a number of predictions of barrier crossing theory. Of particular interest is the form of the reaction rate dependence on the solvent friction,[3–7] and the role of intramolecular and intermolecular vibrational relaxation in determining the reaction rate.[8–11]

The content of the theoretical approaches to barrier crossing has recently been discussed in detail, and here we wish to bring out only a few general points. Firstly, the dependence of reaction rate on solvent friction

can be considered to have two phases. At very low friction the rate of energy accumulation in the reaction coordinate may be rate limiting. If this is the case the reaction rate will increase with increasing friction (collision rate) until the frictional effects resulting from multiple barrier crossing and recrossing begin to dominate. Now the reaction rate "turns over" and begins to ecrease with increasing friction. The low-friction regime is sometimes refrred to as energy controlled, while the high-friction regime is called the diffusion-controlled regime. The two limits correspond to energy exchange and momentum exchange with the surroundings as the dominant process. A second point is that for typical potential surfaces non-Markovian or frequency dependent effects may play an important role in determining the solvent friction.[12–14] The relevant time scale for determining the solvent friction is related to the curvature of the barrier maximum. Simply put, motion of particles over sharp barriers will give rise to memory effects in the surrounding solvent molecules, whereas particles travelling over flat barriers will see the normal, zero frequency, solvent response.

The majority of the theoretical studies have considered one-dimensional systems. However when discussing experimental data on complex molecules it is important to consider the influence of the other degrees of freedom both on the dynamics and on the numerical values of the parameters extracted from the experiments. In our study of diphenyl butadiene (DPB)[15] and stilbene[16] at ultralow liquid viscosities we found that the isomerization rate was still increasing even ar the lowest viscosity reached (0.04 cP). We suggested that for large molecules rapid energy flow from nonreactive to reactive modes will push the position of the turnover to much lower viscosities than expected on the basis of a one-coordinate model. Whether this intramolecular energy flow (IVR) is purely intramolecular, i.e., occurs in the isolated molecule sufficiently rapidly and covers most of the molecular phase space, or can be assisted by collisions is not currently clear. A basic tenet of RRKM theory is that energy randomization is never rate limiting and thus, in molecules for which this is an adequate description, and provided that the molecule is prepared with enough energy to isomerize, the only effect of collisions can be to slow down the rate. This discussion leads us to distinguish two origins for the Kramers turnover. (1) In a thermal (canonical) distribution, collisions can speed up the observed "rate" by restoring the Boltzmann distribution which is distorted by the reaction of the hot molecules. Such a system at zero or low collision rates will in general exhibit nonexponential decay, making the definition of rate problematic. (2) In a microcanonical ensemble in which the total molecular energy content is more than sufficient for isomerization, collisions may speed up the isomerization rate by speeding

the flow of energy from nonreactive to reactive modes if this latter process is rate limiting. Rates of intramolecular vibrational relaxation (IVR) in large molecules with greater than a few thousand wave numbers of energy are expected to be rapid, $\geqslant 10^{12}\,\mathrm{sec}^{-1}$. For example, Felker *et al.*[17],[3] report that IVR times in stilbene are hundreds of picoseconds for $E_x = 1000\,\mathrm{cm}^{-1}$ ($\rho_{\mathrm{vib}} = 113$ per cm^{-1}) and 20–50 psec for $E_x = 1250\,\mathrm{cm}^{-1}$ ($\rho_{\mathrm{vib}} = 428$ per cm^{-1}). Of course the rates do not imply the extent of IVR. Assuming that $k_{\mathrm{IVR}} \propto \rho_{\mathrm{vib}}$, the IVR time scale will not reach 1 psec until $E_x \cong 2000\,\mathrm{cm}^{-1}$. Thus the two types of turnover effects should manifest themselves at different densities. However, the second effect (influence of (IVR) may be difficult to observe experimentally.

The influence of many degrees of freedom on the position of the turnover was taken up theoretically by Zawadzki and Hynes,[18] Nitzan,[19] and Borkovec and Berne,[20] who find that increasing the number of degrees of freedom supresses the influence of vibrational relaxation and shifts the turnover to very low friction values. The multidimensionality of the real system may also influence the form of the friction dependence in the high-friction regime. Hynes and coworkers[21] and Carmeli and Nitzan[22] investigated a two-dimensional model in which a reactive mode is coupled to a nonreactive mode. Both modes feel Markovian friction; however, as the coupling between the modes increases, the influence of friction on the reaction rate becomes weaker. This can make the friction dependence of the reaction rate effectively non-Markovian although for quite a different physical reason than the frequency-dependent medium response discussed above. In a related calculation Agmon[23] has studied the influence of an explicit dependence of reaction rate on motion along an orthogonal coordinate. Here again, a different (weaker) friction dependence is predicted over that suggested by one-dimensional models.

Before describing our results we briefly describe the experimental data obtained to date. Time-resolved spectroscopy has been used to study photochemical isomerization in stilbene,[16,24,25] DPB,[1,15,26] 3,3′-diethyloxadicarbocynanine iodide (DODCI),[2] and binaphthyl.[27,28] Both stilbene and DPB have also been studied in supersonic jet expansions,[29–33] and a comparison between solution and isolated molecules presented.[16,34] In all of the above cases the rate of isomerization was still increasing with decreasing viscosity at the lowest liquid viscosity reached. In contrast to these findings Jonas and coworkers,[35] using a high-pressure nmr technique, found that the rate of cyclohexane ring inversion first increases and then decreases slightly as solvent viscosity is increased. They interpret this

[3] Our directly counted density of states gives substantially larger values than those calculated by Perry *et al.*[57]

behavior as showing qualitative agreement with the predictions of the stochastic models of barrier crossing. In a similar series of experiments, no turnover was observed for difluorocyclohexane.[36] Jones and coworkers suggest that this may result from dielectric friction effects[37] for this polar "probe" molecule in polar solvents.

The form of the viscosity dependence observed in the photochemical isomerization falls into two classes. For stilbene in alkane solvents,[24] DPB in alkanes,[1] DODCI in alcohols (both ground and excited state isomerizations,[2] the reaction rate falls off more slowly with viscosity than predicted from single coordinate theories employing a frequency-independent friction. The experimental results fit well to an empirical expression $k = B/\eta^a$, where $0 < a < 1$. Several authors[2,38] suggested that frequency-dependent friction is responsible for this behavior. Bagchi and Oxtoby,[38] Nitzan and Carmeli,[39] and Zawadzki and Hynes[18] showed that qualitatively a frequency-dependent friction could reproduce the experimental behavior. Rothenberger *et al.*,[24] for the case of stilbene, attempted a quantitative calculation and concluded that although frequency-dependent friction seemed able to describe the experimental results, the value of the curvature of the potential barrier required for the fit was unphysically low. Villaeys *et al.*[66] presented a nonadiabatic model to treat the isomerization rates in liquids and fit the results of Ref. 2.

The second type of behavior is shown by stiff stilbene in alkanes,[24] stilbene in alcohols,[40] and DPB in alcohols.[26] Here the barrier for isomerization is very small (0–1.5 kcal/mol) and the rate of isomerization has a simple inverse viscosity dependence. Keery and Fleming[26] and Velsko *et al.*[2] proposed that for low barriers the potential surface along the reaction coordinate is rather flat and in this case zero-frequency friction is adequate. For stilbene and diphenyl butadiene, the lowering of the internal barrier on going from alkane to alcohol solvents is suggested to result from stabilization of the twisted configuration in polar solvents.[26] The planar form is unaffected by the polarity of the solvent and so the avoided crossing "point"[41] between ^1A_g and ^1B_u potential surfaces is lowered in the polar solvents. If the distance scale remains constant this should also reduce the curvature of the barrier.[2]

2. EXPERIMENTAL METHODS

The technique of time-correlated single photon counting[42,43] with a time resolution of about 20 psec was used to measure fluorescence decays of stilbene and DPB. Experiments were carried out under carefully monitored conditions of temperature and pressure. Details of the experimental procedures can be found elsewhere.[1,16,43]

3. LOW-FRICTION REGION

Studies of the excess energy dependence of the fluorescence lifetimes of stilbene[29,30] and diphenyl butadiene[32] in supersonic expansions have been made. The nonradiative rate (see Figs. 5 and 6), which is presumed to represent isomerization, is constant up to a threshold value and then increases rapidly with increasing excess energy in the isolated molecule. This is quite in accord with the picture given in Fig. 1, with the threshold roughly corresponding to the barrier height. Khundkar *et al.*[44] and Troe and coworkers[45,46] have discussed the energy dependence in terms of RRKM theory.

The observation that molecules with energy less than the barrier height, E_0, do not isomerize, immediately shows that a "Kramers turnover" of type 1 must be observable. Collisions with a thermal buffer gas will activate molecules prepared with $E < E_0$ and enable isomerization to occur. This would be observable, for example, if molecules were prepared with zero excess energy, and then collisions with a buffer gas "turned on." Experimentally it is easier to work with a thermal sample, initially at low pressure so that there are no collisions during the excited state lifetime, and then to increase the buffer gas pressure. In contrast to the single exponential decays observed in solution and in the supersonic jet work, nonexponential decay is observed in the isolated thermal sample. Figure 2 shows the fluorescence decay of stilbene at very low pressures (<0.1 mtorr). It is important to understand the origin of this nonexponential decay in order to perform the appropriate thermal average necessary to compare the supersonic jet data with the solution data. This type of comparison could shed light on whether a turnover of type 2 should be observable. Below we describe a simple model which suggests that the rotational contribution to the density of states should probably be used in performing the thermal average. The model is applied to experimental data on stilbene.

3.1. Origin of Non-Exponential Decay in Thermal Stilbene

We assume that each rovibronic level in the excited singlet state S_1 undergoes single exponential decay as suggested by the outcome of the jet experiments. If E_f is the energy of a rovibronic level in S_1, then we postulate that the collisionless fluorescence intensity for initially thermalized stilbene is given by

$$I_F(t) = \sum_f D(E_f) \exp[-k(E_f)t] \tag{1}$$

where $k(E_f)$ is the total fluorescene rate out of level f and $D(E_f)$ is the pre-

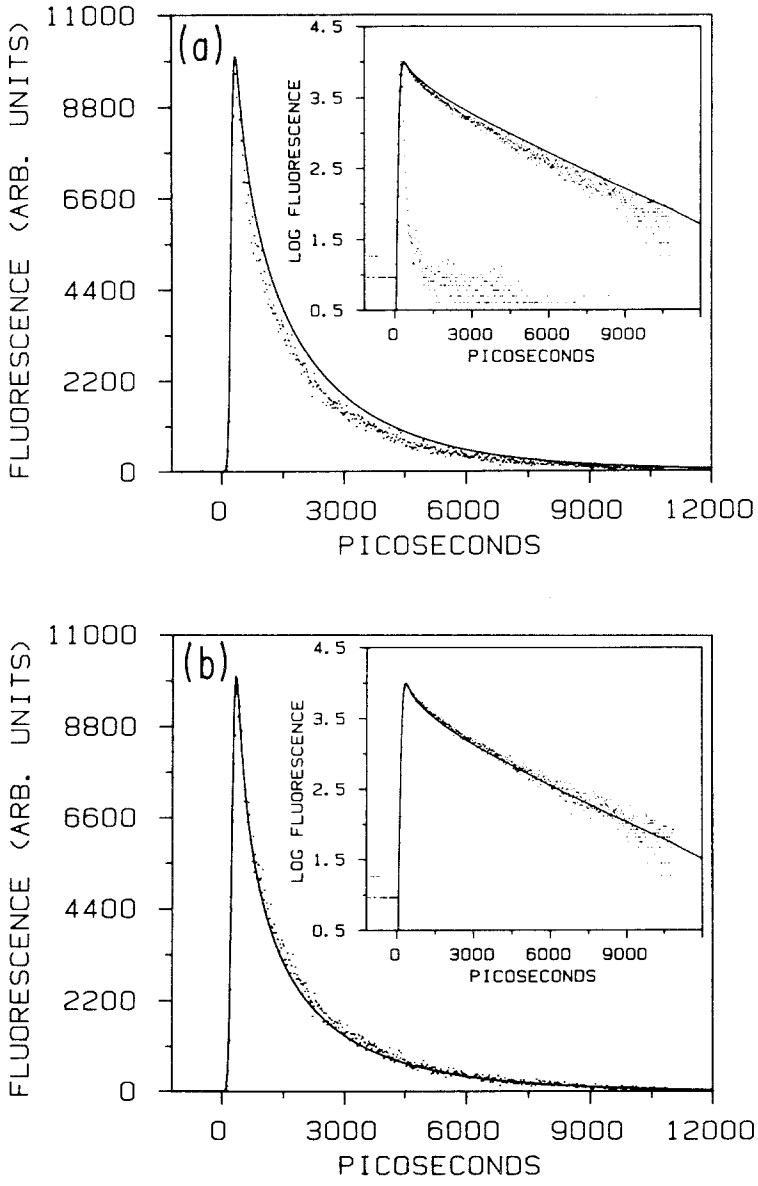

Fig. 2. Collision-free fluorencence decay of the thermalized stilbene vapor. $T = 296$ K, $E_x = 0$. The experimental decay curve (dots) is shown together with the model decay curve (—) calculated according to Eqs. (4) and (5). (a) ρ_g is the vibrational density of states, and (b) ρ_g is the vibrational and rotational density of states [Eq. (7)]. The insets show the experimental and calculated curves on a logarithmic scale. The inset in (a) also contains the instrument function.

isomerization distribution of molecules in S_1 created by the UV excitation pulse. As in previous studies[9,30] we assume

$$k(E_f) = k_r + k_{iso}(E_f) \tag{2}$$

where k_r is the radiative rate, assumed independent of rovibronic level, and $k_{iso}(E_f)$ is the rate of *trans–cis* isomerization for molecules with energy E_f. $D(E_f)$ in Eq. (1) is determined by the Boltzmann distribution in S_0 prior to UV excitation, a set of Franck–Condon factors which determine the allowed transitions from S_0 to S_1 and their relative intensities, and the spectrum of the UV excitation pulse. There may well be other factors influencing the nature of $D(E_f)$, but we shall limit our discussion here to just those listed above. The spectral width of the UV pulse is of the order of 5 to 10 cm^{-1}, which is sufficiently narrow to consider the pulse monochromatic for our purposes.

The Golden Rule calculation of $D(E_f)$ yields a formula for $I_F(t)$ which can be greatly simplified by taking into account the following two important spectroscopic properties of stilbene: (a) Recent spectroscopic studies of jet-cooled stilbene[9a,31] show that only one vibrational mode, ν_{25} (~ 204 cm^{-1} in S_0, $C_e - C_e - \varphi$ symmetric in plane bend[47a]), forms a long progression in both emission and absorption spectra. (b) The frequencies of all 72 normal modes in S_0 are similar to the corresponding frequencies in S_1.[47a,56] These properties suggest that all the modes except ν_{25} undergo relatively little distortion upon excitation to S_1. Setting aside the progression in ν_{25} temporarily, this means that the strongest transitions from S_0 to S_1 are those for which there is no change in the vibrational quantum numbers, with the concomitant result that all the Franck–Condon factors for these transitions are close to unity. Consequently, $D(E_f)$ should be determined primarily by the initial Boltzmann distribution in S_0, if the effects of the progression in ν_{25} on $D(E_f)$ can be neglected.

Consider the case in which the excess vibrational energy E_x (UV energy less the 0–0 transition energy (32 243.5 cm^{-1})[9a,30,31]) is zero. Since the progression in ν_{25} is (approximately) harmonic[9a] and the frequency is about 204 cm^{-1} in S_0, as far as ν_{25} far as ν_{25} is concerned only 25_n^n transitions[4] maintain energy conservation when $E_x = 0$. However, the Franck–Condon factors corresponding to $A_n^{n'}$ for the other modes are nearly all about equal to unity and independent of n'. As a result, the sum over Franck–Condon factors appearing in the Golden Rule formula reduces approximately to the form $C(E_i)\, g(E_i)$, where E_i is the energy of

[4] The symbol A_n^n denotes that upon excitation from S_0 to S_1, the vibrational quantum number of mode A changes from n to m.

the ith level in S_0, $g(E_i)$ is the degeneracy of that level, and $C(E_i)$ is a correction factor of the form

$$C(E_i) = \sum_n{}' \frac{g_n(E_i)}{g(E_i)} F_{nn} \tag{3}$$

where F_{nn} is the Franck–Condon factor for 25_n^n, $g_n(E_i)$ is the number of states with energy E_i in which mode 25 contains n quanta, and $\sum_n'$ denotes that n is summed only over values consistent with energy E_i is S_0. If for all such values of n, F_{nn} were unity, then there would be no correction, i.e., $C(E_i) = 1$. If all the F_{nn} were equal to constant b, then $C(E_i) = b$, which would simply scale $D(E_f)$ be a factor b without altering its shape relative to that obtained with $C(E_i) = 1$. Hence, $C(E_i)$ corrects $g(E_i)$ for the variation in F_{nn} with n. It is quite likely that $C(E_i)$ is a slowly varying function of E_i (e.g., relative to the Boltzmann distribution) at least for energies significantly larger than $\nu_{25} \sim 204\ \text{cm}^{-1}$. For example, it is straightforward to calculate $g_0(E_i)/g(E_i)$, and we find that this ratio varies only about 30% in a smooth manner from the barrier ($\sim 1180\ \text{cm}^{-1}$) to about $6000\ \text{cm}^{-1}$ where the Boltzmann distribution effectively cuts off (296 K). Since the term $n = 0$ accounts for about half (or more) of the states at each value of E_i throughout this range, this suggests (but does not prove) that $C(E_i)$ varies relatively slowly with E_i. Neglecting the more rapid variation of $C(E_i)$ with E_i below the barrier energy has little effect on $I_F(t)$, since molecules initially in such states in S_0 do not isomerize upon excitation to S_1 for the case $E_X = 0$.

Similar results are obtained when E_X is a multiple of $h\nu_{25}$. The case when E_X is not a multiple of $h\nu_{25}$ cannot be treated so simply and will not be considered here. As a consequence of the above discussion, we shall make the assumption that $C(E_i)$ varies slowly with E_i, with the concomitant result that the pre-isomerization distribution in S_1, $D(E_f)$, is simply the initial Boltzmann distribution in S_0 shifted by E_X. This assumption should work best when $E_X = 0$, since then most of the more rapidly varying part of $C(E_i)$ affects only molecules with energy below the isomerization barrier after excitation to S_1. The Golden Rule calculation together with this assumption yields the following equation for $I_F(t, E_X)$:

$$I_F(t, E_X) \propto \exp(-k_r t) \int_0^\infty dE\, \rho_g(E) \exp(-E/k_B T) \exp[-k_{\text{iso}}(E + E_X)t] \tag{4}$$

where $\rho_g(E)$ is the rovibrational density of states in S_0, and k_B is Boltzmann's constant. Comparison with experiment is made possible by

convoluting Eq. (4) with the experimentally determined instrument function, $g(t)$:

$$I_{FC}(t, E_X) = \int_0^t g(t-\tau)\, I_F(\tau)\, d\tau \tag{5}$$

We have calculated the vibrational density of states in S_0, using the normal mode frequencies of stilbene calculated by Warshel,[47a] (and Pierce and Birge[47b] for DPB) via the direct count method[48] from 0 to 10 000 cm^{-1} in increments of 10 cm^{-1}. This range is more than adequate for the temperatures we shall consider here. The isomerization rate constants were obtained by least squares fitting of the function

$$k_{iso}(\bar{\nu}) = A \exp(-B/\bar{\nu}) \tag{6}$$

($\bar{\nu} \equiv$ wave numbers) to the jet rates for stilbene-h_{12} in Table III of Syage, Felker, and Zewail[9b] from 1170 to 2650 cm^{-1}. The results are $A =$ 0.161 $psec^{-1}$ and $B = 9202$ cm^{-1}, with the regression coefficient of fit $r^2 = 0.9946$. We also performed a calculation using the RRKM rates calculated by Troe[45] (his model *C*). The RRKM curve deviates substantially from the exponential model [Eq. (6)] for $E_x > 3000$ cm^{-1}, and should clearly be used for large excess energies. However, for the modest excess energies considered here very little difference was observed in the thermal average decays calculated via the RRKM rate or via Eq. (6).

We have used Eqs. (4) and (5) to calculate fluorescence decay curves corresponding to measurements made at two different temperatures and excess vibrational energies. In order to investigate the possible role of overall rotational motion in stilbene isomerization, we calculated the decay curves with and without the rotational contribution to ρ_g. Figure 2a shows the experimental decay curve for $T = 296$ K, $E_X = 0$ together with the calculated curve obtained using the vibrational contribution to the density of states. Also shown is the relatively narrow instrument function. The experimental and calculated curves were rescaled to a maximum height of 10 000 counts.

The calculated fluorescence decay generally reproduces the shape of the experimental curve in Fig. 2a. The nonexponential shape (see inset) may therefore be attributed to the initial thermal distribution in S_0 prior to excitation, as suggested by Doany *et al.*[49] However, the calculated fluorescence decays slower than the experimental curve. We next consider the extent to which rotational motion may account for this difference.

The rotational contribution to ρ_g may be approximated in the following manner. The overall rotational motion of stilbene is treated classically, since its rotational temperatures are small relative to room tem-

perature, and the angular momentum is initially randomized over a thermal distribution in S_0. We then assume that the rotational motion of isolated stilbene molecules is described by three independent singly degenerate classical rigid rotors.[48] The following equation combines the rotational contribution with the vibrational density of states, $\rho_{g;v}$:

$$\rho_g(E) \propto \int_{E_v=0}^{E} [E - E_v]^{1/2} \rho_{g;v}(E_v)\, dE_v \tag{7}$$

In Fig. 2b the calculated curve now follows the experimental curve almost exactly. It is important to note that this is not a fit to the data; there are no adjustable parameters in the calculation aside from the absolute height of the curve.

We also carried out a calculation for $T = 318$ K, $E_X = 603\ \text{cm}^{-1}$. In this case the correspondence of calculated and measured curves is less than perfect, although the calculation reproduces the rapid initial decay very well. The calculated and measured $1/e$ times for these curves are 0.63 and 0.62 nsec, respectively.

The success of the simple thermal averaging described here should enable clear conclusions to be drawn from a comparison of the isomerization rates in the microcanonical ensembles of isolated molecules and the canonical ensembles of solvated molecules.

3.2. Influence of Buffer Gas Collisons

The qualitative picture behind the nonexponential decay of Fig. 2 is apparent. The hot molecules decay rapidly leading to a progressive cooling of the ensemble. At long times only molecules with insufficient energy to isomerize are left and the decay approaches the radiative lifetime. As buffer gas (methane) pressure is increased the fluorescence decay becomes more nearly single exponential. For pressures above 2 atm the decays are single exponential over two decades; Fig. 3 shows a typical example. As buffer gas pressure is increased the observed lifetime decreases monotonically. Data at 5 atm are presented in Fig. 3 but discussion of this figure is delayed until after the solution data are discussed.

4. HIGH-FRICTION REGIME

We have described experiments in the liquid phase in a number of previous publications,[1,2,15,16] and will only give a brief summary here. First, in order to make a comparison with theory it is necessary to have some experimental measure of friction, or collision rate. For example, in the Kramers expression the simplest approximation to make is that the

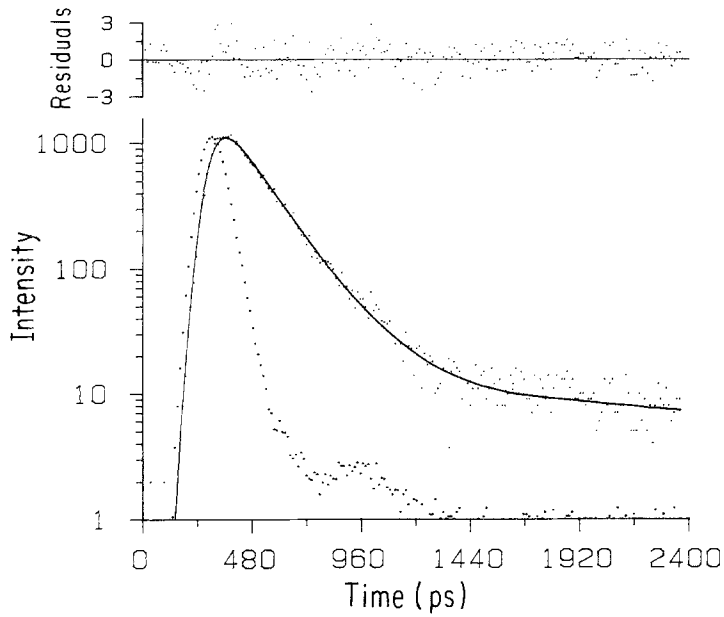

Fig. 3. Fluorescence decay of stilbene vapor in 5 atm of methane gas at 296 K. The solid line is the convolution of a double exponential decay ($\tau_1 = 162$ psec, $\tau_2 = 2216$ psec) with the measured instrument function. The decay is very nearly single exponential since the prefactor of the short component is 99.3%, The weighted residuals are shown on the upper curve ($x^2 = 1.01$) and the instrument function has been scaled to the fluorescence decay.

momentum correlation time is inversely proportional to the solvent shear viscosity. We call this the hydrodynamic approximation to Kramers theory. At this level of approximation expressions for barrier crossing rate can be written in the form

$$k = F(\eta) \exp(-E_0/RT) \tag{8}$$

The prefactor $F(\eta)$ has little or no intrinsic temperature dependence The prefactor $F(\eta)$ has little or no intrinsic temperature dependence if the explicit temperature dependene of the viscosity is taken into account. Thus if E_0 (equivalent to the barrier height in the isolated molecule aside from a small pV correction term) is known, then a plot of $F(\eta)$ vs. η may be constructed from data taken (1) at a fixed temperature (T) and pressure (P) for a series of solvents which span the desired range of η, (2) at a fixed P and solvent as a function of T, and (3) at a fixed T and solvent as a function of P. If the value of E_0 is insensitive to solvent, temperature, and pressure the same value of $F(\eta)$ should be obtained no matter how the particular value of the viscosity was reached. Values of E_0 are obtained from the temperature dependence at fixed viscosity—"isoviscosity plots".[1]

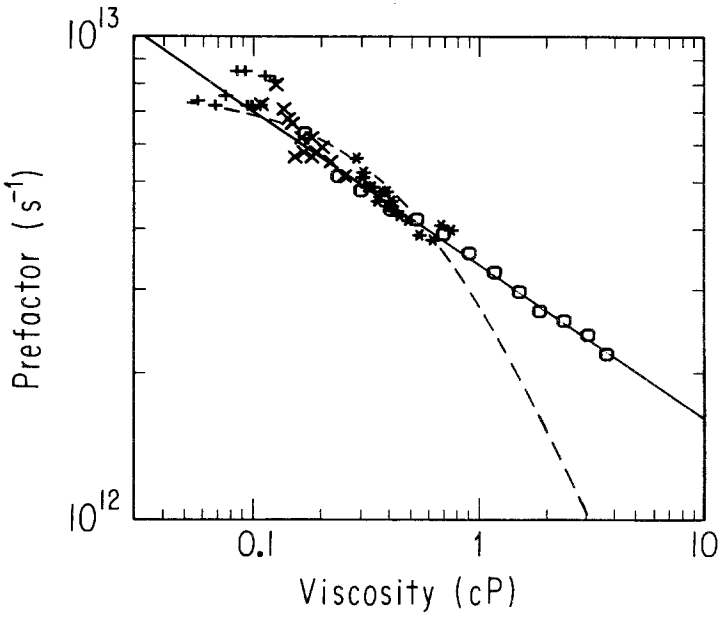

Fig. 4. The prefactor, $F(\eta)$, versus shear viscosity for stilbene in normal alkanes. ○, Higher alkanes at room temperature from Ref. 24; *, in hexane at varying temperature; ×, in liquid propane; +, in liquid ethane. The solid line is a fit to expression (10) and the dashed line is a fit to expression (9).

Figure 4 shows a typical $F(\eta)$ vs. $\log \eta$ plot for stilbene in normal alkanes. The viscosity is varied by nearly two orders of magnitude (0.06 to 4 cP) by a combination of solvent and temperature change. The circles indicate different normal alkanes at room temperature, the other symbols refer to temperature dependent studies in particular solvents. To a good approximation the same rate $[F(\eta)]$ is obtained no matter how the particular values of η was reached.

In a similar study on diphenyl butadiene, measurements were also carried out in octane up to pressure of 3 kbar.[1] Again the $F(\eta)$ data so obtained were indistinguishable from those obtained by temperature or solvent variation.

Two fits to the data are shown in Fig. 4. The dashed line is a two-parameter fit to the hydrodynamic form of Kramers equation

$$F(\eta) = A/(B/\eta)\{[1 + (B/\eta)^2]^{1/2} - 1\} \tag{9}$$

where $A = (\omega/2\pi)Q^{\ddagger}/Q'$ and $B/\eta = 2\,\omega_B \tau_v$. Here ω is the frequency of the initial (reactant) well, $Q^{\ddagger}/Q'$ is the ratio of vibrational partition functions

in the transition state and the reactant state (the prime indicated that the reaction coordinate partition function has been removed from Q), ω_B is the curvature of the barrier, and τ_v is the momentum relaxation time along the reaction coordinate. The qualitative failure of (9) to fit the data is also characteristic of our data for DPB in alkanes,[1] and DODCI excited and ground states in alcohols.[2] A similar failure is also found in 1(1-pyrene)3-(4-dimethylaminophenyl) propane (PDMAPP) by Russo and Thistlewaite.[51]

In our previous studies we found that the empirical relation

$$F(\eta) = B/\eta^a \tag{10}$$

with $0 < a < 1$ fit all our data very well. The solid line in Fig. 4 shows a fit to (10) with $B = 3.5 \times 10^{12}\ \text{sec}^{-1}$ and $a = 0.32$. Russo and Thistlethwaite[51] also found (10) fit their data well with $a = 0.53$. The value of a can be taken as a measure of the deviation from simple Smoluchowski limit ($a = 1$) behavior; the smaller the value of a, the larger the deviation from expressions of the form of Eq. (9).

In contrast to our findings Miller and Eisenthal[28] found a good fit to (9), but not the Smoluchowski limit of (9) for binaphthyl in linear alcohol solvents.

Table I summarizes the available barrier crossing data for stilbene,[16,24] stiff stilbene,[24] DPB,[1,15] DODCI,[2] PDMAPP,[51] binaphthyl,[28] and Fav 2R.[52] Note that the overall rotational reorientation of DODCI is very well described by the Stokes–Einstein expression.[50] Within a given molecular system both the value of the prefactor and the value of a correlate with the barrier height. It is this correlation which initially led us to propose that the frequency dependence of the solvent response was the reason for the failure of the Kramers expression (9) to fit most of the experimetal data.[2]

This suggestion was taken up by several authors who applied the Grote–Hynes theory,[12] which gives the rate as

$$k = (\lambda_R/\omega_B)k_{\text{TST}} \tag{11a}$$

$$\lambda_R = \frac{\omega_B{}^2}{\lambda_R + \hat{\zeta}(\lambda_R)/\mu} \tag{11b}$$

where $\hat{\zeta}(\lambda_R)$ is the Laplace transform of the time-dependent friction $\zeta(t)$. In applying equation (11) to the experimental results there seem to be two ways to proceed. One can either use a model of $\hat{\zeta}(\lambda_R)$ and attempt to fit the data, or use an experimental value for ω_B and extract the frequency-dependent friction from the data. Bagchi and Oxtoby[53] and Rothenberger *et*

Table I. Summary of Isomerization Data

System	Barrier height (kcal/mol)	Prefactor at 1 cP (sec^{-1})	a^a	Ref.
Stilbene				
Alkanes	3.5	3.5×10^{12}	0.32	16, 24, 64
Alcohols	<1	2×10^{10}–3×10^{11}	0.6	40
Thermal vapor	3.3	4×10^{11}	—	57
Stiff stilbene				
Alkanes	1.5	1.2×10^{12}	$\sim 1.0^b$	24
DPB				
Alkanes	4.7	1.6×10^{12}	0.66	1, 15
Alcohols	~0.5	1.5×10^{10}	0.92^b	26
DODCI				
Alcohols (ground state)	13.7	4×10^{12}	0.26	2
Alcohols (excited state)	2.7	8×10^{11}	0.43	2
Rotation	—	$\sim 10^{10}$	0.99	50
PDMAPP				
Alkanes	2.4	1.5×10^{10}	0.53	51
Binaphthyl Alcohols	1.3	7×10^{11}	Fits full Kramers equation	27, 28
Fav 2R Alcohols	~0.2	9×10^{10}	0.98^b	52

[a] From fits to Eq. (10).
[b] Also fit well to Smoluchowski limit of Eq. (9).

al.[24] have used the former method using experimental data on the viscoelastic response of solvents. Grote *et al.*[18] used an analytical expression for $\tilde{\zeta}(\lambda_R)$ based on molecular dynamics calculations in liquid argon. All three calculations find a dependence of rate on shear viscosity of the form of Eq. (10). Rothenberger *et al.*[24] attempted a quantitative fit for stilbene and concluded that the value of ω_B required for the fit was unphysically low. It is not currectly clear whether this arises from the inappropriateness of the theory or the difficulty in constructing an appropriate frequency-dependent friction from available data.

An alternative approach might be to use the RRKM fits of Troe and coworkers[45,46] for stilbene and DPB to define ω and the partition function ratio in Eq. (9). In other words, one can assume $k_\infty = k_{TST}$, where k_∞ is calculated according to

$$k_\infty = \int_{E_0}^{\infty} f(E)\, k(E)\, dE \tag{12}$$

Here $f(E)$ is the thermal equilibrium distribution.[45] This approach assumes that IVR is complete in the isolated molecule (for energies greater than E_0), an assumption that we feel requires further testing, given the IVR time scales suggested by Felker *et al.*[17] (see Introduction). In general the influence of entropy on the prefactor should be taken into account. Changes in vibrational frequencies in the transition state may make a very substantial contribution.[16] If the RRKM condition is satisfied this is taken into account by the above procedure. In the condensed phase however, other factors such as displaced volume changes between reactant and transition states may also make a significant contribution to the prefactor in solution.[54]

It is possible that the fractional viscosity dependence [expression (10)] is a general signature of non-Markovian effects in the friction and it is of interest to discuss other possible origins of memory effects in these systems. Hynes and coworkers[21] and Carmeli and Nitzan[22] studied the influence of friction on the rate of barrier crossing for a model in which a reactive mode is coupled to a nonreactive mode. Both modes feel Markovian friction. Both studies conclude that the coupling between the modes reduces the influence of friction on the rate. In Fig. 1 of Ref. 22 the rate becomes essentially independent of friction at high coupling strength. This implies that fractional viscosity dependences would be expected at intermediate coupling strength. In a related calculation Agmon and Hopfield[23] have pointed out that if the barrier crossing rate depends explicitly on the motion of other coordinates, then a fractional viscosity dependence may arise. Further study of the influence of other coordinates and more realistic models for the shape of the potential in the transition state region are needed before the importance of frequency-dependent friction can be assessed.

5. BARRIER CROSSING OVER THE WHOLE DENSITY RANGE

In order to compare the rates of barrier crossing in isolated, high pressure gas, and solvated molecules it is necessary to define a universal parameter against which rates can be plotted. Maneke *et al.* has proposed the use of the inverse diffusion coefficient for this purpose.[25] For a comparison of isolated molecules with the other systems Perry *et al.*[57] proposed the use of the vibrational energy content, E_v. This quantity is defined in one of three ways. (1) For isolated, jet-cooled molecules, E_v is simply the excess energy E_x above the zero point acquired in the excitation process. (2) For isolated, thermalized molecules E_v is the sum of the

average vibrational energy calculated from Eq. (13) and E_x. (3) Finally, for solvated molecules E_v is given directly by (13)

$$\langle E_v \rangle = Nk_B \sum_i \frac{h\nu_i/k_B}{\exp(h\nu_i/k_B T) - 1} \tag{13}$$

Figures 5 and 6 show plots of k vs. E_v for stilbene and DPB, respectively. A notable feature of these plots is that the rate of isomerization in DPB is very similar in low-viscosity solvents to the rates observed in the supersonic jet. In stilbene the solution rates are very much faster than the jet rates. The solid lines are thermal averages calculated using the jet data for stilbene[9b,30] and the RRKM results of Troe *et al.* for DPB[46] in Eqs. (4) and (5). For stilbene the solution data lie above the thermal average, while for DPB the thermal average gives similar rates to those measured in liquid ethane. We will return to this difference below.

Figure 7 shows the dependence of the observed isomerization rate for stilbene, plotted as a function of inverse diffusion coefficient. Following Maneke *et al.*[25] the diffusion coefficient, D, was obtained from

$$\frac{kT}{\eta D} \cong 3\pi d_{ST}[1 - \exp(-[M]/[M]_{crit})] \tag{14}$$

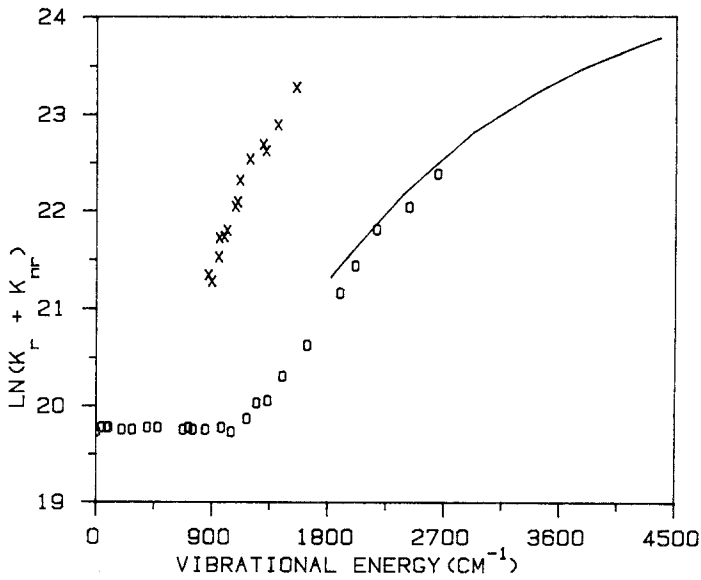

Fig. 5. Rates of photoisomerization of stilbene as a function of vibrational energy. The abscissa corresponds to the average vibrational energy as defined in the text. 0, Jet Results from Ref. 9; ×, in liquid ethane. The solid line is the natural log of the $1/e$ times of the thermal gas decay calculated according to Eqs. (4)–(7) for the thermal vapor at 296 K as a function of excess energy (see text).

where η is the viscosity and $[M]_{crit}$ is the critical density. We used $d_{ST} = 3.7$ Å for the diameter of the phenyl ring and obtained the viscosities and densities for methane and ethane from data in Refs. 58–60. The isomerization rate rises, then falls with increasing D^{-1}, and it is tempting to claim that Fig. 7 represents a clear demonstration of the energy-controlled and diffusion-controlled regions of a barrier-crossing process. Unfortunately, as usual, things are more complicated than this simple picture. Maneke *et al.*[25] have observed a substantial red shift in the $S_0 - S_1$ absorption spectrum as a function of ethane gas pressure. The absorption maximum shifts by about 1200 cm^{-1} between 0.13 and 42.2 bar. A differential shift between the B_u and A_g states will clearly alter the barrier height (position of avoided crossing). Nothing is currectly known about the shift of the A_g state with pressure, however it seems to be common lore that it will be less sensitive to environment than the B_u state. In this case, the red

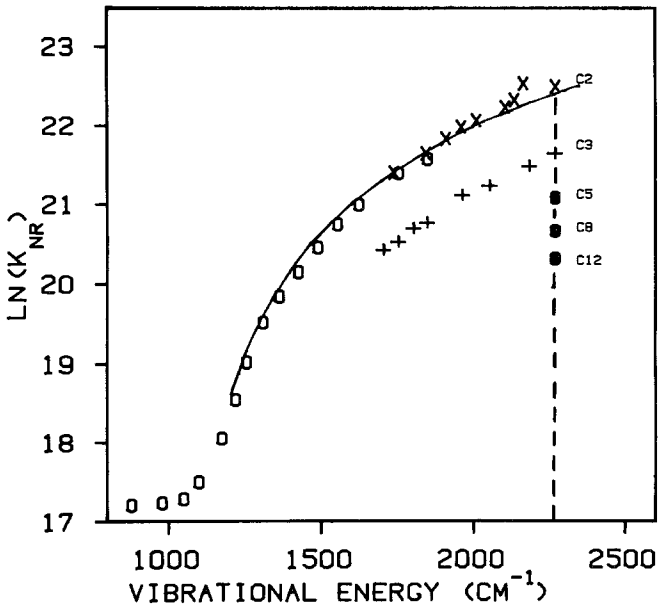

Fig. 6. Rates of photoisomerization of diphenyl butadiene as a function of vibrational energy. The abscissa corresponds to the average vibrational energy as defined in the text. 0, Jet results from Ref. 32; ×, in liquid ethane; +, in liquid propane. The vertical line shows the influence of the solvent viscosity at 24°C ($E_v = 2270$ cm^{-1}). The solid line is the natural log of the $1/e$ times of the thermal gas decay calculated according to Eqs. (4) and (5) with k_r set to zero and no excess energy (see text). The nonradiative rate as a function of energy required in Eq. (4) was obtained by third-order polynomial interpolation of the RRKM rates in Ref. 46. The normal mode frequencies required in the density of states calculation (see text) were obtained from Ref. 47b.

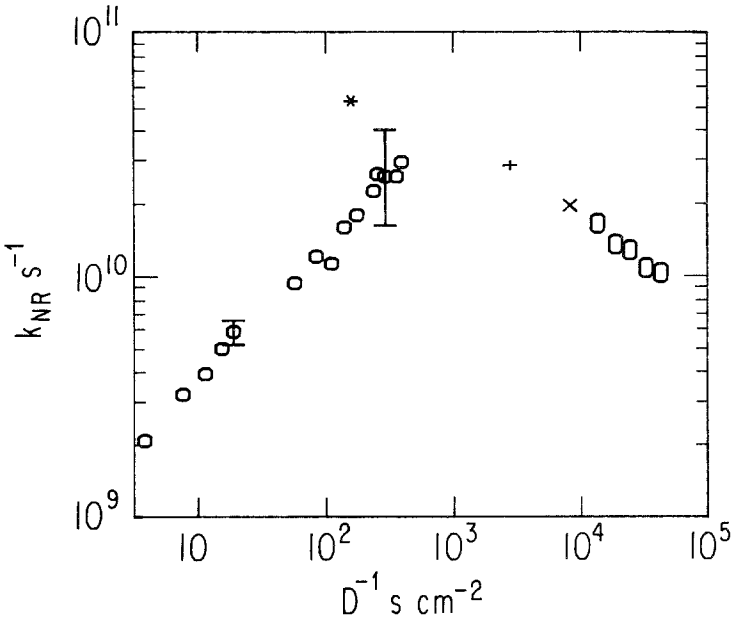

Fig. 7. Room temperature photoisomerization rates for stilbene vs. the inverse of the diffusion coefficients in gaseous and liquid alkanes. ○, In methane varying the pressure; *, in gaseous ethane at 329 K from Ref. [25; +, in liquid ethane; ×, in liquid propane; 0, in higher alkanes from Ref. 24. The maximum pressure in gaseous methane studied was 90 atm. The uncertainty of the short lifetimes is greater than for lifetimes longer than $\cong 100$ psec because of the difficulty of determining an exact instrument response function in our high-pressure cell. The error bars are estimates based on deconvolution using instrument functions obtained in different manner. We used 3.7×10^8 sec^{-1} for the radiative rate in gaseous methane. The excitation wavelength in gaseous methane was 310 nm. Note that the spectral shift observed by Maneke *et al.*[25] implies that excess energy of the initial state increases with increasing gas pressure.

shift of the ground state B_u adsorption will lower the barrier and accelerate the rate. The spectrum shows negligible shift up to 10 bar,[25] and since we find about an order of magnitude increase in rate over this range, it is clear that the entire rise in Fig. 7 cannot be attributed to pressure-dependent shift in the potential surface. On the other hand (J. Troe, private communication) DPB exhibits similar spectral shifts and yet the isolated molecule rate is much closer to the solution value. Manake *et al.*[25] have also modeled the isomerization including the influence of density-dependent solvent shifts of the barrier energy. Recently, Sundstrom and Gillbro[64] obtained a smaller E_0 value in the normal alkane series C_{12}–C_{16} than obtained in the lower alkanes.[16] This is consistent with the assumption that the solvent cage shifts of E_0 are more pronounced in these conditions.[25]

One way to compare the solution phase results to the isolated molecule results without neglecting the influence of barrier energy changes is to compare the preexponential factors. Consider the k_∞ values determined by Troe *et al.*[45,46] and the Arrhenius prefactors determined in liquid ethane.

Stilbene:

$$k_\infty = 8.3 \times 10^{11} \exp(-1250 \text{ cm}^{-1}\, hc/kT) \text{ sec}^{-1}$$

$$k_{NR} = 1.7 \times 10^{13} \exp(-1220 \text{ cm}^{-} hc/kT) \text{ sec}^{-1}$$

DPB:

$$k_\infty = 8.3 \times 10^{11} \exp(-1000 \text{ cm}^{-1}\, hc/kT) \text{ sec}^{-1}$$

$$k_{NR} = 5.5 \times 10^{13} \exp(-1854 \text{ cm}^{-1}\, hc/kT) \text{ sec}^{-1}$$

In the stilbene case, the activation energy in solution is only slightly less than that determined from the RRKM fit and in DPB the value is significantly larger. There are substantial increases in the frequency factor for both stilbene and DPB on going from the gas phase to liquid ethane. (It is interesting that the frequency factors for k_∞ in stilbene and DPB are identical). Thus changes in observed rate between gas and liquid phases can not be explained only in terms of barrier height changes. The increase in prefactor on solvation may be related to several factors: (1) collisional assistance of intramolecular vibrational redistribution, (2) conformational entropy effects (activation volume effects),[54b] and (3) changes in low-frequency modes in solution. A further possible complication is that the process may be nonadiabatic at low collison rates and become adiabatic at higher collision rates.[9b] It is clear that further studies are necessary before a complete interpretation of Fig. 7 can be given.

6. SUMMARY

Qualitatively the photochemical isomerizations of stilbene and DPB depend on friction in the manner suggested by Kramers in 1940. The energy-controlled region has been directly observed in high-pressure gases for stilbene by ourselves and by Hochstrasser and coworkers.[61] Quantitative description of the rate dependence is hampered by a number of uncertainties: (1) the shift (if any) in the shape of the potential surface as a function of interaction with the surrounding medium, (2) the degree of nonadiabaticity (if any) of the process in the low-pressure regime, (3) the way in which the multidimensional nature of the potential surface influences the dynamics, (4) the method of generating a reliable frequency-dependent friction for molecular solvents.

ACKNOWLEDGMENTS

This work was suported by a grant from the National Science Foundation. S.H.C. was supported in part by a Xerox Foundation Physical Chemistry grant. We thank Professor Jürgen Troe for some very helpful discussions.

REFERENCES

1. S. P. Velsko and G. R. Fleming, *J. Chem. Phys.* **76**:3553 (1982).
2. S. P. Velsko, D. H. Waldeck, and G. R. Fleming, *J. Chem. Phys.* **78**:249 (1983).
3. B. Carmeli and A. Nitzan, *Phys. Rev. Lett.* **51**:233 (1983).
4. J. L. Skinner and P. G. Wolynes, *J. Chem. Phys.* **72**:4913 (1983).
5. P. Hanggi and U. Weiss, *Phys. Rev. A* **29**:2265 (1984).
6. B. J. Matkowsky, Z. Schuss, and C. Tier, *J. Stat. Phys.* **35**:443 (1984).
7. J. T. Hynes, in *The Theory of Chemical Reaction Dynamics*' M. Baer, ed. (Chemical Rubber, Boca Roton, Florida, 1985).
8. P. M. Felker and A. H. Zewail, *Chem. Phys. Lett.* **108**:303 (1984).
9. (a) J. A. Syage, P. M. Felker, and A. H. Zewaill, *J. Chem. Phys.* **81**:4685 (1984); (b) J. A. Syage, P. M. Felker, and A. H. Zewail, *J. Chem. Phys.* **81**:4706 (1984).
10. B. J. Berne, *Chem. Phys. Lett.* **107**:131 (1984).
11. K. F. Freed and A. Nitzan, in *Energy Storage and Redistribution in Molecules*, J. Hinze, ed. (Plenum, New York, 1983).
12. R. F. Grote and J. T. Hynes, *J. Chem. Phys.* **73**:2715 (1980); R. F. Grote, G. van der Zwan, and J. T. Hynes, *J. Phys. Chem.* **88**:4767 (1984).
13. P. Hänggi and F. Mojtabai, *Phys. Rev. A* **26**:1168 (1982); P. Hänggi, *J. Stat. Phys.* **30**:401 (1983).
14. B. Carmeli and A. Nitzan, *J. Chem. Phys.* **79**:393 (1983).
15. S. H. Courtney and G. R. Fleming, *Chem. Phys. Lett.* **103**:443 (1984).
16. S. H. Courtney and G. R. Fleming, *J. Chem. Phys.* **83**:215 (1985).
17. P. M. Felker, W. R. Lambert, and A. H. Zewail, *J. Chem. Phys.* **82**:3003 (1985).
18. R. F. Grote, G. Van der Zwan, and J. T. Hynes, *J. Phys. Chem.* **88**:4676 (1984).
19. A. Nitzan, *J. Chem. Phys.* **82**:1614 (1985).
20. M. Borkovec and B. J. Berne, *J. Chem. Phys.* **82**:794 (1985).
21. R. F. Grote and J. T. Hynes, *J. Chem. Phys.* **74**:4465 (1981); *J. Chem. Phys.* **75**:2191 (1981); G. von der Zwan and J. T. Hynes, *J. Chem. Phys.* **77**:1295 (1982); G. von der Zwan and J. T. Hynes, *Chem. Phys.* **90**:21 (1984).
22. B. Carmeli and Nitzan, *Chem. Phys. Lett.* **106**:329 (1984).
23. N. Agmon and J. J. Hopfield, *J. Chem. Phys.* **78**:6947 (1983); N. Agmon, *Chem. Phys. Lett.* (in press).
24. G. Rothenberger, D. K. Negus, and P. M. Hochstrasser, *J. Chem. Phys.* **79**:5360 (1983).
25. G. Maneke, J. Schroeder, J. Troe, and F. Voss, *Ber. Bunsenges. Phys. Chem.* **89**:896 (1985).
26. K. M. Keery and G. R. Fleming, *Chem. Phys. Lett.* **93**:322 (1982).
27. C. V. Shank, E. P. Ippen, O. Teschke, and K. B. Eisenthal, *J. Chem. Phys.* **67**:5547 (1977).
28. D. Millar and K. B. Eisenthal, *J. Chem. Phys.* (submitted).
29. J. A. Syage, W. R. Lambert, P. M. Felker, A. H. Zewail, and R. M. Hochstrasser, *Chem. Phys. Lett.* **88**:266 (1982).
30. T. J. Majors, U. Even, and J. Jortner, *J. Chem. Phys.* **81**:2330 (1984).
31. T. S. Zwier, E. Carrasquillo, and D. H. Levy, *J. Chem. Phys.* **78**:5493 (1983).

32. J. F. Shepanski, B. W. Keelan, and A. H. Zewail, *Chem. Phys. Lett.* **103**:9 (1983).
33. L. A. Heimbrook, B. E. Kohler, and T. A. Spiglanin, *Proc. Natl. Acad. Sci. U.S.A.* **80**:4580 (1983).
34. S. H. Courtney, G. R. Fleming, L. R. Khundkar, and A. H. Zewail, *J. Chem. Phys.* **80**:4559 (1984).
35. D. Hasha, T. Eguchi, and J. Jonas, *J. Am. Chem. Soc.* **104**:2290 (1982).
36. J. Ashcraft, M. Besnard, V. Aquado, and J. Jonas, *Chem. Phys. Lett.* **110**:420 (1984).
37. (a) G. van der Zwan and J. T. Hynes, *J. Chem. Phys.* **76**:2993 (1982); (b) G. van der Zwan and J. T. Hynes, *J. Chem. Phys.* **78**:4174 (1983); (c) G. van der Zwan and J. T. Hynes, *Chem. Phys. Lett.* **101**:367 (1983).
38. B. Bagchi and D. W. Oxtoby, *J. Chem. Phys.* **78**:2735 (1983).
39. B. Carmeli and A. Nitzan, *J. Chem. Phys.* **80**:3596 (1984).
40. V. Sundström and T. Gillbro, *Chem. Phys. Lett.* **109**:538 (1984).
41. G. Orlandi and W. Siebrand, *Chem. Phys. Lett.* **30**:352 (1975).
42. R. J. Robbins, G. R. Fleming, G. S. Beddard, G. W. Robinson, P. J. Thistlewaite, and G. J. Woolfe, *J. Am. Chem. Soc.* **102**:6171 (1980); G. R. Fleming, W. T. Lotshaw, R. J. Gulotty, M. Chang, and J. W. Petrich, in *Photochemistry and Photobiology: Proceedings of the Intl. Conference, January 1983, University of Alexandria, Egypt*, A. H. Zewail, ed. (Harwood, Chur, 1983).
43. M. C. Chang, S. H. Courtney, A. J. Cross, R. J. Gulotty, J. W. Petrich, and G. R. Fleming, *Anal. Biochim.*, (in press).
44. L. R. Khundkar, R. A. Marcus, and A. H. Zewail, *J. Phys. Chem.* **87**:2473 (1983).
45. J. Troe, *Chem. Phys. Lett.* **114**:241 (1985).
46. J. Troe, A. Amirav, and J. Jortner, *Chem. Phys. Lett.* **115**, 245 (1985).
47. (a) A. Warshel, *J. Chem. Phys.* **62**:214 (1975); (b) B. M. Pierce and R. R. Birge, *J. Chem. Phys.* **86**:2651 (1982).
48. P. J. Robinson and K. A. Holbrook, *Unimolecular Reactions* (Wiley, New York, 1972).
49. F. E. Doany, B. I. Greene, Y. Liang, D. K. Negus, and R. M. Hochstrasser, in *Picosecond Phenomena II* (Springer, New York, 1980).
50. D. H. Waldeck and G. R. Fleming, *J. Phys. Chem.* **85**:2614 (1981).
51. S. Russo and P. J. Thistlewaite, *Chem. Phys. Lett.* **106**:91 (1984).
52. C. J. Tredwell and A. D. Osborne, *J. Chem. Soc. Faraday Trans. 2* **76**:1627 (1980).
53. B. Bagchi and D. W. Oxtoby, *J. Chem. Phys.* **78**:2735 (1983).
54. (a) G. W. Robinson, W. A. Jalenak, and D. Statman, *Chem. Phys. Lett.* **110**:135 (1984); (b) D. Statman and G. W. Robinson, *J. Chem. Phys.* **83**:655 (1985).
55. D. W. Oxtoby, *J. Chem. Phys.* **70**:2605 (1979).
56. R. H. Dyck and D. S. McClure, *J. Chem. Phys.* **36**:2326 (1962).
57. J. W. Perry, N. F. Scherer, and A. H. Zewail, *Chem. Phys. Lett.* **103**:1 (1983).
58. H. J. M. Hanley, W. M. Haynes, and R. D. McCarty, *J. Phys. Chem. Ref. Data* **6**:597 (1977).
59. R. D. McCarty, *Cryogenics* **14**:276 (1974).
60. H. J. M. Hanley, K. E. Gubbins, and S. Murad, *J. Phys. Chem. Ref. Data* **6**:1168 (1977).
61. M. Lee, G. R. Holtom, and R. M. Hochstrasser, *Chem. Phys. Lett.* **118**:359 (1985).
62. B. I. Greene and T. W. Scott, *Chem. Phys. Lett.* **106**:399 (1984).
63. M. Sumitani and K. Yoshihara, *Bull. Chem. Soc. Jpn.* **55**:85 (1982).
64. V. Sundström and T. Gillbro, *Ber. Bunsenges, Phys. Chem.* **89**:222 (1985).
65. (a) A. A. Villaeys, A. Boeglin, and S. H. Lin, *Chem. Phys. Lett.* **116**:210 (1985); (b) A. A. Villaeys, A. Boeglin, and S. H. Lin, *J. Chem. Phys.* **82**:4044 (1985).
66. H. A. Kramers, *Physica* 7:284 (1940).